Biochimica et Biophysica Acta 1810 (2011) 612–619

Contents lists available at ScienceDirect

Biochimica et Biophysica Acta

journal homepage: www.elsevier.com/locate/bbagen

Analogs of 5-(substituted benzylidene)hydantoin as inhibitors of tyrosinase and melanin formation

Young Mi Ha [a,1], Jin-Ah Kim [b,1], Yun Jung Park [b], Daeui Park [a], Ji Min Kim [a], Ki Wung Chung [a], Eun Kyeong Lee [a,c], Ji Young Park [b], Ji Yeon Lee [b], Hye Jin Lee [b], Jeong Hyun Yoon [a], Hyung Ryong Moon [b,*], Hae Young Chung [a,**]

[a] College of Pharmacy, Pusan National University, Kumjeong-Gu, Busan 609-735, Republic of Korea
[b] Laboratory of Medicinal Chemistry, College of Pharmacy, Pusan National University, Busan 609-735, Republic of Korea
[c] Research Center, Dongnam Institute of Radiological and Medical Sciences, Busan 619-953, Republic of Korea

ARTICLE INFO

Article history:
Received 13 January 2011
Received in revised form 28 February 2011
Accepted 2 March 2011
Available online 11 March 2011

Keywords:
5-(substituted benzylidene)hydantoin derivatives
Tyrosinase inhibitory activity
Docking study with mushroom tyrosinase
Antimelanogenesis

ABSTRACT

Background: Many tyrosinase inhibitors find application in cosmetics and pharmaceutical products for the prevention of the overproduction of melanin in the epidermis. A series of 5-(substituted benzylidene) hydantoin derivatives **2a**–**2k** were prepared, and their inhibitory activities toward tyrosinase and melanin formation were evaluated.
Methods: The structures of the compounds were established using ^{1}H and ^{13}C NMR spectroscopy and mass spectral analyses. All the synthesized compounds were evaluated for their mushroom tyrosinase inhibition activity.
Results: The best results were obtained for compound **2e** which possessed hydroxyl group at R^2 and methoxy group at R^3, respectively. We predicted the tertiary structure of tyrosinase, simulated its docking with compound **2e** and confirmed that this compound interacts strongly with mushroom tyrosinase residues as a competitive tyrosinase inhibitor. In addition, we found that **2e** inhibited melanin production and tyrosinase activity in B16 cells.
Conclusions: Compound **2e** could be considered as a promising candidate for preclinical drug development in skin hyperpigmentation applications.
General significance: This study will enhance understanding of the mechanism of tyrosinase inhibition and will contribute to the development of effective drugs for use hyperpigmentation.

1. Introduction

Human skin pigmentation occurs as a result of the accumulation of melanin in the epidermis; melanin is produced by melanocytes within specialized organelles called melanosomes. Melanogenesis occurs through a complex pathway involving enzymatic and chemical reactions that are restricted to melanosomes, the melanocyte-specific organelles containing all the components required to synthesize the pigment. The conversion of tyrosine to melanin requires tyrosinase, a copper-containing protein (Fig. 1). This tyrosinase (monophenol monooxygenase, EC 1.14.18.1) plays the central role in melanogenesis as the key enzyme that catalyzes the hydroxylation of tyrosine to form 3,4-dihydroxyphenylalanine (L-DOPA), and L-DOPA to DOPA quinone [1,2]. A large number of dermatological disorders are characterized by the increased production and accumulation of melanin; such disorders include abnormal pigmentations such as freckles, age spots, and melasma, which can be serious [3,4].

Many tyrosinase inhibitors find application in cosmetics and pharmaceutical products for the prevention of the overproduction of melanin in the epidermis. Because of its key role in melanogenesis, tyrosinase is an attractive target in the search for various kinds of depigmenting agents [5–8]. In recent years, various tyrosinase inhibitors have been reported such as azelaic acid [9], ascorbic acid derivatives [10], arbutin [11], kojic acid [12], hydroxystilbene compounds such as resveratrol [13–15], and polyphenolic compounds

Abbreviations: AcOH, Acetic acid; ANOVA, Analysis of variance; CaH_2, Calcium hydride; CO_2, Carbon dioxide; $CDCl_3$, Deuterated chloroform; L-DOPA, L-3,4-dihydroxyphenylalanine; DMSO, Dimethyl sulfoxide; MTT, 3-(4,5-Dimethylthiazol-2-yl)-2,5-diphenyltetrazolium bromide; DMEM, Dulbecco's modified eagle's medium; FBS, Fetal bovine serum; HCl, Hydrogen chloride; NMDA, N-methyl-D-aspartic acid; NMR, Nuclear magnetic resonance; NaOAc, Sodium acetate; TLC, Thin-layer chromatography; PBS, Phosphate-buffered saline; PDB, Protein data bank

* Correspondence to: H.R. Moon, Laboratory of Medicinal Chemistry, College of Pharmacy, Pusan National University, Busan 609–735, Republic of Korea. Tel.: +82 51 510 2815; fax: +82 51 513 6754.
** Correspondence to: H.Y. Chung, Molecular Inflammation Research Center for Aging Intervention (MRCA), College of Pharmacy, Pusan National University, Kumjeong-Gu, Busan 609-735, Republic of Korea. Tel.: +82 51 510 2814; fax: +82 51 518 2821.
E-mail addresses: mhr108@pusan.ac.kr (H.R. Moon), hyjung@pusan.ac.kr (H.Y. Chung).
[1] Y.M. Ha and J.-A. Kim contributed equally to this article.

0304-4165/$ – see front matter © 2011 Elsevier B.V. All rights reserved.
doi:10.1016/j.bbagen.2011.03.001

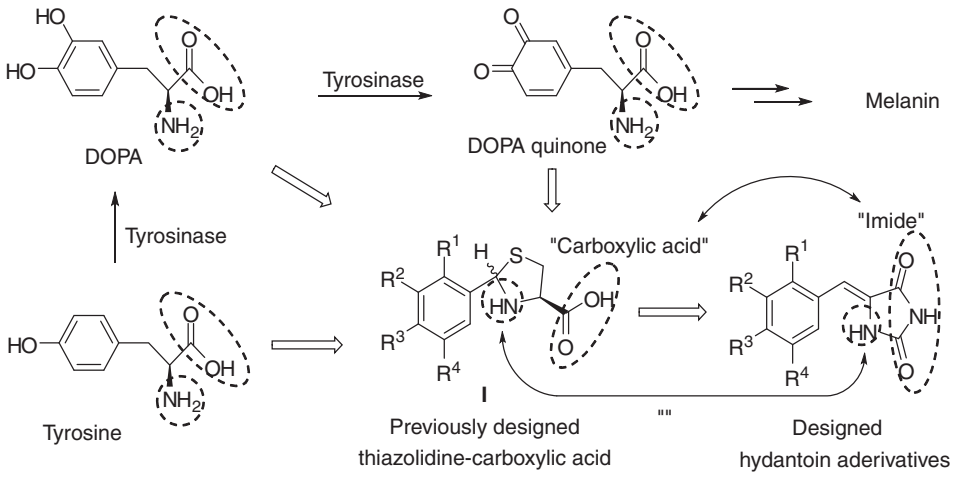

Fig. 1. Rationale for the design of the 5-(substituted benzylidene)hydantoin derivatives.

[16–18]. A previous study has shown that 3,4-dihydroxyacetophenone and 4,4′-dihydroxybiphenyl have strong anti-tyrosinase activities that inhibits melanogenesis [19,20]. We have also reported that hydroxy substituted 2-phenyl-naphthalenes as resveratrol analogs, 5-(6-hydroxy-2-naphthyl)-1,2,3-benzenetriol, 6-(3-hydroxyphenyl)-2-naphthol, and 4-(6-hydroxy-2-naphtayl-1,3-bezendiol) inhibit tyrosinase activity and reduced melanin biosynthesis in B16 cells, which indicates that these compounds could find use as depigmentation agents. We have also found several potent tyrosinase inhibitors in natural materials; these have a potent inhibitory effect on melanogenesis [18,20,21] and the microphthalmia-associated transcription factor [19].

Recently, our laboratory synthesized thiazolidine-carboxylic acid derivatives **I** on the basis of the structures of the substrates and products of tyrosinase, and we found that some of them showed significant inhibitory activities against tyrosinase (Fig. 1). The carboxylic acid and amine (NH) functionalities in **I** appeared to play an important role in the inhibition of tyrosinase activity. Our interest in an alternative structure capable of replacing thiazolidine-carboxylic acid led us to study the hydantoin template. We considered that the imide group of the hydantoin would play the role of the carboxylic acid of **I** at the active site of tyrosinase because the hydrogen atoms of both the imide and the carboxylic acid could commonly act as acidic protons and because the imide and the carboxylic acid both possessed a carbonyl group capable of interacting with amino acid residues present at the active site of tyrosinase (Fig. 1). Hydantoin derivatives have been identified as anticancer [22,23], anticonvulsant [24], anti-inflammatory [25,26], anti-HIV [27], antidiabetic [28], antimuscarinic [29,30], antiulcer [31], antiarrythmic [32], and antihypertensive agents [33]. They have also been found to act as serotonin and fibrinogen receptor antagonists [34,35], inhibitors of the glycine binding site of the NMDA receptor [36], and antagonists of leukocyte cell adhesion, acting as allosteric inhibitors of the protein–protein interaction [37]. Hydantoin derivatives also show antiproliferative effects toward human carcinoma cells [38]. However, their effects on tyrosinase and skin melanogenesis are not yet known.

In this study, eleven 5-(substituted benzylidene)hydantoin derivatives, **2a**–**2k** were synthesized, and their mushroom tyrosinase inhibitory activities were evaluated. Among these derivatives, **2e** exhibited the highest inhibition of the L-DOPA oxidase activity of mushroom tyrosinase at a concentration of 20 μM. This work was designed to characterize the effects of **2e** on mushroom tyrosinase activity and on tyrosinase activity and melanin levels in B16 melanoma cells (B16 cells). We also predicted the tertiary structure of tyrosinase, and simulated its docking with **2e**.

2. Materials and methods

2.1. Experimental

2.1.1. General

Melting points are uncorrected. ^{1}H and ^{13}C NMR spectra were recorded on Varian Unity INOVA 400 and Varian Unity AS 500 instruments. Chemical shifts are reported with reference to the respective residual solvent or deuteriated peaks (δ_H 3.30 and δ_C 49.0 for CD_3OD, δ_H 7.27 and δ_C 77.0 for $CDCl_3$). Coupling constants are reported in Hertz. The abbreviations used are as follows: s (singlet), d (doublet), t (triplet), dd (doublet of doublets), and br s (broad singlet). All the reactions described below were performed under an argon or nitrogen atmosphere and were monitored by thin-layer chromatography (TLC). All anhydrous solvents were distilled over CaH_2 or Na/benzophenone before use.

2.1.2. Method A: general procedure I for the synthesis of substituted benzylidene-hydantoin analogs (*2a–2d, 2f–2g, and 2i*)

A suspension of substituted benzaldehydes (2.42–7.70 mmol) and hydantoin (1.1 equiv.) in piperidine (1 ml/4 mmol benzadehyde) was heated at reflux for duration between 30 min and 6 h. The reaction mixture was cooled, and water (20 times the volume of piperidine used) was added at 60 °C. Any traces of tarry material were removed by filtration. The filtrate was acidified with 12 N HCl at room temperature. The mixture was kept at room temperature for a few hours. The precipitates generated were then filtered off using a Buchner funnel and washed with cold water. They were then dried under reduced pressure, and the substituted benzylidene-hydantoin products (yields: 9.7–79%) were obtained.

2.1.3. Method B: general procedure II for the synthesis of substituted benzylidene-hydantoin analogs (*2e, 2h, and 2k*)

A suspension of substituted benzaldehydes (1.08–1.28 mmol) and hydantoin (1.1 equiv.) in EtOH (2–4 ml) and H_2O (2–4 ml) was heated to 80 °C. After the reaction mixture had been heated at the same temperature for 30 to 50 h, the precipitates formed were filtered off using a Buchner funnel and washed with water to remove excess hydantoin and methylene chloride or ethyl acetate, depending on the property of the substituted benzaldehydes remaining, to give the title products (yields: 11.4–71.4%).

2.1.4. Method C: synthesis of (Z)-5-(4-hydroxy-3,5-dimethoxybenzylidene) imidazolidine-2,4-dione (*2j*)

A suspension of syringaldehyde (300 mg, 1.65 mmol), hydantoin (198 mg, 1.98 mmol), and sodium acetate (405 mg, 4.94 mmol) in

acetic acid (1.6 ml) was heated at reflux for 24 h. The precipitate generated was filtered using a Buchner funnel and washed with methylene chloride and a small amount of water. After being drying under reduced pressure, the title product (192.9 mg, 44.3%) was obtained.

*2.1.4.1. (Z)-5-(4-Hydroxybenzylidene)imidazolidine-2,4-dione (**2a**).* Pale yellowish solid; reaction time, 30 min; yield, 78.5%; melting point, >300 °C; ^{1}H NMR (500 MHz, DMSO-d_6) δ 11.10 (s, 1H, NH), 10.30 (s, 1H, NH), 9.84 (s, 1H, OH), 7.46 (d, 2 H, J = 8.0 Hz, 2′-H, 6′-H), 6.77 (d, 2 H, J = 8.0 Hz, 3′-H, 5′-H), 6.34 (s, 1 H, vinylic H); ^{13}C NMR (100 MHz, DMSO-d_6) δ 166.3 (C4), 158.7 (C4′), 156.3 (C2), 131.9 (C2′, C6′), 126.0 (C5), 124.5 (C1′), 116.4 (C3′, C5′), 110.0 (benzylic C); LRMS(ES) m/z 203 (M-H)$^-$.

*2.1.4.2. (Z)-5-(2-Hydroxybenzylidene)imidazolidine-2,4-dione (**2b**).* Yellowish solid; reaction time, 2 h; yield, 50.3%; melting point, 265.5–268.4 °C; ^{1}H NMR (500 MHz, DMSO-d_6) δ 11.17 (s, 1H, NH), 10.29 (s, 1H, NH), 10.08 (s, 1H, OH), 7.54 (d, 1H, J = 8.0 Hz, 6′-H), 7.16 (td, 1H, J = 1.0, 8.0 Hz, 4′-H), 6.88 (d, 1H, J = 8.0 Hz, 3′-H), 6.82 (t, 1H, J = 8.0 Hz, 5′-H), 6.67 (s, 1H, vinylic H); ^{13}C NMR (100 MHz, DMSO-d_6) δ 166.3 (C4), 156.5 (C2′), 156.1 (C2), 130.6 (C4′), 130.0 (C6′), 127.7 (C5), 120.7 (C1′), 120.0 (C5′), 116.1 (C3′), 104.4 (benzylic C); LRMS(ES) m/z 203 (M-H)$^-$.

*2.1.4.3. (Z)-5-(4-Methoxybenzylidene)imidazolidine-2,4-dione (**2c**).* Yellowish solid; reaction time, 4 h; yield, 17.4%; melting point, 241.8–242.9 °C; ^{1}H NMR (400 MHz, DMSO-d_6) δ 11.13 (s, 1 H, NH), 10.40 (s, 1H, NH), 7.55 (d, 2 H, J = 8.8 Hz, 2′-H, 6′-H), 6.92 (d, 2 H, J = 8.8 Hz, 3′-H, 5′-H), 6.35 (s, 1H, vinylic H), 3.75 (s, 3 H, 4′-OCH$_3$); ^{13}C NMR (100 MHz, DMSO-d_6) δ 166.3 (C4), 160.1 (C4′), 156.3 (C2), 131.8 (C2′, C6′), 126.7 (C5), 126.1 (C1′), 115.0 (C3′, C5′), 109.3 (benzylic C), 55.9 (4′-OCH$_3$); LRMS(ES) m/z 217 (M-H) $^-$.

*2.1.4.4. (Z)-5-(3,4-Dihydroxybenzylidene)imidazolidine-2,4-dione (**2d**).* Brown solid; reaction time, 30 min; yield, 68.7%; melting point, >300 °C; ^{1}H NMR (400 MHz, CD$_3$OD) δ 6.92–6.89 (m, 2H, 2′-H, 6′-H), 6.80 (d, 1H, J = 8.8 Hz, 5′-H), 6.43 (s, 1 H, vinylic H); ^{13}C NMR (100 MHz, CD$_3$OD) δ 166.6 (C4), 156.4 (C2), 146.8 (C4′), 145.6 (C3′), 125.7 (C5), 125.1 (C1′), 121.7 (C6′), 116.4 (C5′), 115.6 (C2′), 111.7 (benzylic C); LRMS(ES) m/z 219 (M-H) $^-$.

*2.1.4.5. (Z)-5-(3-Hydroxy-4-methoxybenzylidene)imidazolidine-2,4-dione (**2e**).* Pale green yellow solid; reaction time, 40 h; yield, 36%; melting point, 250.7–253.4 °C; ^{1}H NMR (400 MHz, DMSO-d_6) δ 11.10 (br s, 1H, NH), 10.33 (br s, 1H, NH), 9.01(s, 1 H, OH), 7.05 (dd, 1 H, J = 2.0, 8.4 Hz, 6′-H), 6.97 (d, 1 H, J = 2.0 Hz, 2′-H), 6.89 (d, 1 H, J = 8.4 Hz, 5′-H), 6.25 (s, 1 H, vinylic H), 3.77 (s, 3 H, 4′-OCH$_3$); ^{13}C NMR (100 MHz, DMSO-d_6) δ 166.3 (C4), 156.3 (C2), 149.0 (C4′), 147.1 (C3′), 126.9 (C5), 126.4 (C1′), 121.9 (C6′), 117.4 (C2′), 112.7 (C5′), 109.9 (benzylic C), 56.3 (4′-OCH$_3$); LRMS(ES) m/z 233 (M-H)$^-$.

*2.1.4.6. (Z)-5-(4-Hydroxy-3-methoxybenzylidene)imidazolidine-2,4-dione (**2f**).* Green yellow solid; reaction time, 30 min; yield, 74%; melting point, 249.2–251.6 °C; ^{1}H NMR (500 MHz, DMSO-d_6) δ 11.11 (s, 1H, NH), 10.40 (s, 1H, NH), 9.42 (s, 1H, OH), 7.09 (d, 1H, J = 1.5 Hz, 2′-H), 7.06 (dd, 1H, J = 1.5, 8.5 Hz, 6′-H), 6.78 (d, 1H, J = 8.5 Hz, 5′-H), 6.35 (s, 1H, vinylic H), 3.82 (s, 3 H, 3′-OCH$_3$); ^{13}C NMR (100 MHz, DMSO-d_6) δ 166.3 (C4), 156.4 (C2), 148.4 (C3′), 148.2 (C4′), 126.1 (C5), 125.0 (C1′), 124.1 (C6′), 116.4 (C5′), 113.8 (C2′), 110.5 (benzylic C), 56.4 (3′-OCH$_3$); LRMS(ES) m/z 233 (M-H)$^-$.

*2.1.4.7. (Z)-5-(3-Ethoxy-4-hydroxybenzylidene)imidazolidine-2,4-dione (**2g**).* Ocherous solid; reaction time, 30 min; yield, 79%; melting point, 253.0–255.4 °C; ^{1}H NMR (400 MHz, DMSO-d_6) δ 11.08 (s, 1H, NH), 10.36 (s, 1H, NH), 9.32 (s, 1H, OH), 7.06 (d, 1H, J = 2.4 Hz, 2′-H), 7.03 (dd, 1H, J = 2.0, 8.4Hz, 6′-H), 6.76 (d, 1H, J = 8.0 Hz, 5′-H), 6.30 (s, 1H, vinylic H), 4.06 (q, 2H, J = 6.8 Hz, CH$_3$*CH*$_2$-), 1.30 (t, 3 H, J = 6.8 Hz, *CH*$_3$CH$_2$-); ^{13}C NMR (100 MHz, DMSO-d_6) δ 166.3 (C4), 156.4 (C2), 148.6 (C3′), 147.6 (C4′), 126.1 (C5), 125.0 (C1′), 124.2 (C6′), 116.5 (C5′), 115.3 (C2′), 110.4 (benzylic C), 64.7 (3′-O*CH*$_2$), 15.4 (CH$_2$*CH*$_3$); LRMS(ES) m/z 247 (M-H) $^-$.

*2.1.4.8. (Z)-5-(2,4-Dimethoxybenzylidene)imidazolidine-2,4-dione (**2h**).* White solid; reaction time, 30 h; yield, 71.4%; melting point, 234.1–237.2 °C; ^{1}H NMR (500 MHz, DMSO-d_6) δ 11.09 (s, 1H, NH), 10.28 (s, 1H, NH), 7.55 (d, 1H, J = 8.5 Hz, 6′-H), 6.60 (s, 1H, vinylic H), 6.59 (d, 1H, J = 2.5 Hz, 3′-H), 6.54 (dd, 1H, J = 2.0, 8.5 Hz, 5′-H), 3.83 (s, 3H, OCH$_3$), 3.79 (s, 3 H, OCH$_3$); ^{13}C NMR (100 MHz, DMSO-d_6) δ 166.3 (C4), 161.8 (C4′), 159.3 (C2′), 156.2 (C2), 130.8 (C6′), 126.7 (C5), 114.9 (C1′), 106.2 (benzylic C), 103.7 (C5′), 98.9 (C3′), 56.4 (2′-OCH$_3$), 56.1 (4′-OCH$_3$); LRMS(ES) m/z 247 (M-H) $^-$.

*2.1.4.9. (Z)-5-(3,4-Dimethoxybenzylidene)imidazolidine-2,4-dione (**2i**).* Pale yellowish solid; reaction time, 6 h; yield, 9.7%; melting point, 271.3–273.9 °C; ^{1}H NMR (500 MHz, DMSO-d_6) δ 11.15 (s, 1H, NH), 10.48 (s, 1 H, NH), 7.18 (dd, 1H, J = 1.5, 8.0 Hz, 6′-H), 7.11 (d, 1H, J = 2.0 Hz, 2′-H), 6.95 (d, 1 H, J = 8.5 Hz, 5′-H), 6.37 (s, 1H, vinylic H), 3.81 (s, 3H, OCH$_3$), 3.77 (s, 3H, OCH$_3$); ^{13}C NMR (100 MHz, DMSO-d_6) δ 166.3 (C4), 156.4 (C2), 150.0 (C3′), 149.4 (C4′), 126.8 (C5), 126.3 (C1′), 123.7 (C6′), 113.2 (C5′), 112.4 (C2′), 109.9 (benzylic C), 56.3 (OCH$_3$), 56.2 (OCH$_3$); LRMS(ES) m/z 247 (M-H)$^-$.

*2.1.4.10. (Z)-5-(4-Hydroxy-3,5-dimethoxybenzylidene)imidazolidine-2,4-dione (**2j**).* Yellow solid; reaction time, 24 h; yield, 44.3%; melting point, 266.0–268.5 °C; ^{1}H NMR (500 MHz, DMSO-d_6) δ 11.13 (s, 1H, NH), 10.50 (s, 1H, NH), 8.81 (s, 1H, OH), 6.82 (s, 2H, 2′-H, 6′-H), 6.35 (s, 1H, vinylic H), 3.81 (s, 6H, 3′-OCH$_3$, 5′-OCH$_3$); ^{13}C NMR (100 MHz, DMSO-d_6) δ 166.3 (C4), 156.5 (C2), 148.7 (C3′, C5′), 137.4 (C4′), 126.2 (C5), 123.8 (C1′), 110.8 (benzylic C), 108.0 (C2′, C6′), 56.8 (3′-OCH$_3$, 5′-OCH$_3$); LRMS(ES) m/z 263 (M-H)$^-$.

*2.1.4.11. (Z)-5-(3,4,5-Trimethoxybenzylidene)imidazolidine-2,4-dione (**2k**).* Yellow solid; reaction time, 50 h; yield, 11.4%; melting point, 266.3–267.2 °C; ^{1}H NMR (400 MHz, DMSO-d_6) δ 11.19 (br s, 1H, NH), 10.58 (br s, 1H, NH), 6.80 (s, 2H, 2′-H, 6′-H), 6.33 (s, 1 H, vinylic H), 3.80 (s, 6H, 3′-OCH$_3$, 5′-OCH$_3$), 3.64 (s, 3H, 4′-OCH$_3$); ^{13}C NMR (100 MHz, DMSO-d_6) δ 166.2 (C4), 156.5 (C2), 153.7 (C3′, C5′), 138.6 (C4′), 129.2 (C1′), 127.9 (C5), 109.7 (benzylic C), 107.6 (C2′, C6′), 60.7 (4′-OCH$_3$), 56.7 (3′-OCH$_3$, 5′-OCH$_3$); LRMS(ES) m/z 277 (M-H)$^-$.

2.2. Materials

Mushroom tyrosinase, L-tyrosine [3-(4-hydroxyphenyl)]-L-alanine (*S*)-2-amino-3-(4-hydroxyphenyl) propionic acid), kojic acid [5-hydroxy-2-(hydroxymethyl)-4*H*-pyran-4-one], and α-MSH (alpha-melanocyte stimulating hormone) were purchased from Sigma Chemical Co. (St. Louis, MO, USA).

2.3. Methods

2.3.1. Cell culture

B16 cells (obtained from the Korean Cell Line Bank) were cultured in Dulbecco's Modified Eagle's Medium (DMEM; Gibco, Carlsbad, CA, USA) with 10% fetal bovine serum (FBS; Gibco) and penicillin/streptomycin (100 IU·50 μg^{-1}·ml^{-1}) in a humidified atmosphere containing 5% CO_2 at 37 °C. B16 cells were cultured in 24-well plates for melanin quantification and enzyme activity assays.

2.3.2. Cell viability

Cell survival was quantified through a colorimetric 3-(4,5-dimethylthiazol-2-yl)-2,5-diphenyltetrazolium bromide (MTT) assay

that measured the mitochondrial activity in viable cells. This method is based on the conversion of MTT (Sigma) to MTT-formazan crystals by a mitochondrial enzyme and has been described previously [39]. Briefly, cells seeded at a density of 3×10^4/cell in a Corning 48-well plate (Corning, NY, USA) were allowed to adhere overnight; the culture medium was then replaced with fresh serum-free DMEM. MTT was freshly prepared at 5 mg·ml^{-1} in phosphate-buffered saline (PBS) solution. 500 μl aliquots of the MTT stock solution were added to each well, and the plate was incubated at 37 °C for 4 h in a humidified 5% CO_2 incubator. After 4 h, the medium was removed. 500 μl of EtOH-DMSO (1:1 solution) was added to each well to dissolve the formazan. After 10 min, the optical density of each well was measured spectrophotometrically using a 560 nm filter.

The results from three experiments are shown.

2.3.3. Assay for the measurement of inhibitory effects on mushroom tyrosinase

Mushroom was used as the source of tyrosine for the entire study. Tyrosinase activity was determined as described previously with minor modifications [40]. Briefly, 20 μl of an aqueous mushroom tyrosinase solution (1000 units) was added to a 96-well microplate (Nunc, Denmark), in a 200 μl assay mixture containing 1 mM L-tyrosine solution and 50 mM phosphate buffer (pH 6.5). The assay mixture was incubated at 25 °C for 30 min. Following incubation, the amount of dopachrome produced in the reaction mixture was determined spectrophotometrically at 492 nm (OD_{492}) using a microplate reader (Hewlett Packard, Palo Alto, CA, USA). IC_{50}, or inhibitory concentration 50, is the concentration of a compound that inhibits a standard 50% response. IC_{50} values are derived from the X-axis on a curve of inhibitor concentration versus product formation and determined from the alignment of the dose-response curve on the dependent *Y*-axis. In the present study, dose-dependent inhibition experiments were performed in triplicate to determine the IC_{50} values of the compounds. According to the inhibition percentages of the three doses in each experiment, the log-linear curves and their equations were determined. The individual IC_{50} values were then calculated as the concentration when the *Y*-axis was equal to 50% inhibition. The results from three experiments are shown.

2.3.4. Kinetic analysis of tyrosinase inhibition

Various concentration of L-tyrosine (0.25 to 2 mM) as a substrate, 20 μl of aqueous mushroom tyrosinase solution (1000 units), and 50 mM potassium phosphate buffer (pH 6.5), with or without test samples (1.25 and 20.0 μM of **2e**), were added to a 96-well plate in a total volume of 200 μl. Using a microplate reader, the initial rate of dopachrome formation from the reaction mixture was determined by the increase in absorbance at a wavelength of 492 nm per minute ($\Delta OD_{492}\cdot min^{-1}$). The Michaelis constant (K_m) and maximal velocity (V_{max}) of the tyrosinase activity were determined from a Lineweaver–Burk plot at various L-tyrosine concentrations [34]. A modification of the Michaelis–Menten equation was required to describe the reaction kinetics due to competitive inhibition by the compounds together with substrate inhibition by L-tyrosine. The results from three experiments are shown.

2.3.5. Assay of murine tyrosinase activity

Tyrosinase activity was estimated by measuring the rate of L-DOPA oxidation [41]. Cells were placed in 24-well dishes at a density of 5×10^4 cells·ml^{-1}. B16 cells were incubated in the presence or absence of 100 nM α-MSH and they were then treated for 24 h with various concentrations of **2e** (0–10 μM). The cells were washed and lysed in 100 μl of 50 mM sodium phosphate buffer (pH 6.5) containing 1% Triton X-100 (sigma) and 0.1 mM PMSF (phenylmethylsulfonyl fluoride), and then frozen at −80 °C for 30 min. After being thawed and mixed, the cellular extracts were clarified by centrifugation at 12000 rpm for 30 min at 4 °C. An 8 μl sample of the supernatant and 20 μl of L-DOPA (2 mg·ml^{-1}) were placed in a 96-well plate, and the absorbance at 492 nm was recorded every 10 min for 1 h at 37 °C using an ELISA plate reader. The final activity is expressed as ΔO. D.·min^{-1} for each set of conditions. The results from three experiments are shown.

2.3.6. Determination of melanogenesis in B16 cells

The melanin content was determined using a modification of the method of Bilodeau et al. [42]. In the present study, the amount of melanin was used as the index of melanogenesis. B16 cells (5×10^4) were transferred to 24-well dishes and incubated in the presence or absence of 100 nM α-MSH. The cells were then incubated for 24 h with various concentrations of **2e** (0–10 μM). The samples were washed twice with PBS and were then dissolved in 100 μl of 1N NaOH. The samples were incubated at 60 °C for 1 h and mixed to solubilize the melanin. The absorbance at 405 nm was compared with a standard curve for synthetic melanin. The results from three experiments are shown.

2.3.7. Homology modeling of tyrosinase

A three-dimensional model of *Lentinula edodes* (mushroom) tyrosinase comprising 618 amino acids was built using the SWISS-MODEL [43] program and on the basis of homology modeling [44]. The SWISS-MODEL program automatically provides an all-atom model using alignments between the query sequence and known homologous structures. Known homologous structures of tyrosinase from the Protein Data Bank (PDB) (http://www.pdb.org) were used as the structural templates. The PDB: 1BT3 was a suitable structural template (15% sequence identity).

2.3.8. In silico docking of tyrosinase and novel inhibitor candidates

Among the many tools available for *in silico* protein-ligand docking, DOCK6 is the most commonly used because of its automated docking capability. The program performs ligand docking using a set of predefined 3D grids of the target protein through a systemic search technique [45].

We describe the structures of the novel inhibitor candidates in Figs. 1 and 4. To prepare for the docking procedure, we performed the following steps: (1) conversion of the 2D structures into 3D structures; (2) calculation of charges; and (3) addition of hydrogen atoms using the ChemOffice program (www.cambridgesoft.com).

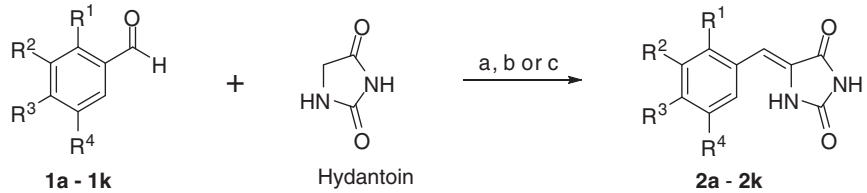

Scheme 1. Synthesis of the target compounds, 5-(substituted benzylidene)hydantoin derivatives (**2a**–**2k**); reagents and conditions: **method A**: i) piperidine, reflux, 30 min–6 h; ii) water at 60 °C; iii) filtration; iv) 12N HCl for **2a**–**2d**, **2f**–**2g**, and **2i**; **method B**: EtOH/H_2O (1:1), 80 °C, 30–50 h for **2e**, **2 h**, and **2k**; **method C**: NaOAc, AcOH, reflux, 24 h for **2j**.

2.4. Statistical analysis

The inhibition of tyrosinase activity is expressed as a percentage of inhibition, based on the equation $100-[(A\times100)/B]$, where A is OD_{492} with a test sample, and B is OD_{492} without a test sample. The data collected have a mean standard error ($n=3$). The statistical significance of the differences between groups was determined by one-factor analysis of variance (ANOVA) followed by Fisher's protected least significant difference post hoc test. Values of $^{*}p<0.05$ were considered statistically significant.

3. Results and discussion

Hydantoins and their derivatives constitute a group of pharmaceutical compounds with anticonvulsant and antiarrhythmic properties, and are also used against diabetes. Eleven 5-(substituted benzylidene) hydantoin derivatives, **2a–2 k** were obtained through three synthetic methods (Scheme 1). Initially, method A using piperidine as a base, was employed for the synthesis of some of the target compounds. However, when using alkoxy-benzaldehydes **1c** and **1i** (Table 1) as starting materials, the purification and solidification processes were difficult, and the yields were low because of gum materials generated. Therefore, method B, which did not use base, was attempted for the preparation of **2e**, **2h**, and **2k**, and the desired products were obtained more easily and in higher purity. Both method A and method B were tried for the synthesis of **2j**, but the ^{1}H NMR spectra showed that the product was not pure, even though it looked like one spot in the TLC results. In this case, method C, using NaOAc and AcOH, was attempted, and the desired hydantoin derivative **2j** was afforded without any impurities in moderate yield. For the preparation of 5-(2,4-dihydroxybenzylidene) hydantoin and 5-(3,5-dihydroxybenzylidene)hydantoin from 2,4-dihydroxybenzaldehyde and 3,5-dihydroxybenzaldehyde, the three aforementioned methods were attempted, but none were successful. The synthetic reactions for the substituted benzylidene-hydantoin analogs gave **2a–2d, 2f–2 g**, and **2i** in 9.7–79% yields using method A, **2e**, **2h**, and **2k** in 11.4–71.4% yields using method B, and **2j** in 44.% yield using method C (Scheme 1 and Table 1). The structures of the synthesized compounds were determined by ^{1}H and ^{13}C NMR spectroscopy and mass spectroscopic analyses.

Table 1
Substitution pattern of the substituted benzylidene-hydantoin derivatives **2a–2k.**

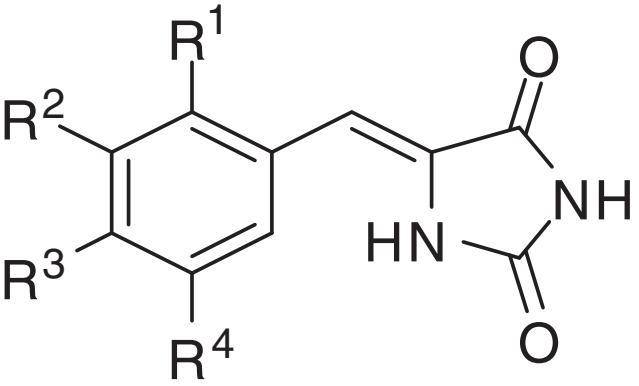

Compound	R^1	R^2	R^3	R^4	Yield (%)	Reaction time (hour)	Tyrosinase inhibition (%)[a]
2a	H	H	OH	H	78.5	0.5	38.95 ± 0.36
2b	OH	H	H	H	50.3	2	NI
2c	H	H	OMe	H	17.4	4	19.85 ± 0.61
2d	H	OH	OH	H	68.7	0.5	NI
2e	H	OH	OMe	H	36.0	40	86.54 ± 0.49
2f	H	OMe	OH	H	74.0	0.5	17.33 ± 0.41
2g	H	OEt	OH	H	79.0	0.5	5.16 ± 0.31
2h	OMe	H	OMe	H	71.4	30	21.61 ± 0.50
2i	H	OMe	OMe	H	9.7	6	17.17 ± 0.40
2j	H	OMe	OH	OMe	44.3	24	21.59 ± 0.48
2k	H	OMe	OMe	OMe	11.4	50	41.79 ± 0.55
Kojic acid							41.89 ± 0.95

Values represent means ± S.E. of three experiments, NI (no inhibition).
[a] Tyrosinase inhibition was measured using L-tyrosine as the substrate at 20 μM.

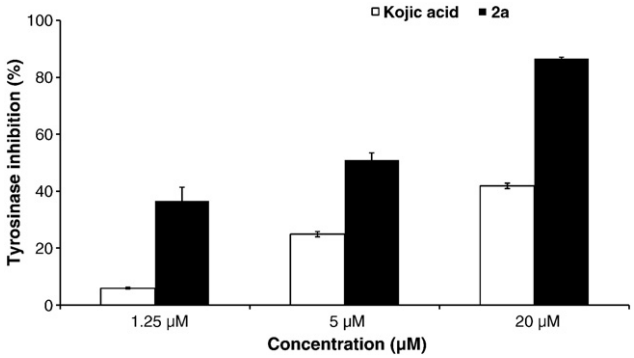

Fig. 2. Dose-dependent inhibitory effects of **2e** and kojic acid on tyrosinase activity. Tyrosinase activity was measured using L-tyrosine as the substrate. Results are expressed as percentage of control, and each column represents the mean ± S.E. of three determinations. The optical density value of control at 492 nm was 0.486 ± 0.007.

The inhibitory activities of the synthesized compounds were examined using mushroom tyrosinase, as described previously, with minor modification [40]. The inhibitory activities of these newly synthesized compounds were compared to that of kojic acid as a reference control, and the results are shown in Table 1 and Fig. 2. In terms of the structure-activity relationships, compound **2d** with two substituents (the hydroxy group at R^2 and R^3, respectively) on the phenyl ring has a similar structure to DOPA, which also has hydroxyl groups at R^2 and R^3 on the phenyl ring, but **2d** showed no mushroom tyrosinase inhibition. Further, compound **2a**, with a hydroxyl group at R^3 on the phenyl ring, has a similar structure to tyrosine, one of the substrates of tyrosinase, but it showed poor mushroom tyrosinase inhibition. Compound **2e**, containing a hydroxyl group at R^2 and a methoxy group at R^3, showed the highest inhibitory activity against mushroom tyrosinase, but **2f**, with these groups inverted (a methoxy group at R^2 and a hydroxyl group at R^3), and **2i** (with methoxy groups at R^2 and R^3) showed little inhibitory activity. Among the newly synthesized compounds, we further investigated the bioactivities of **2e**, because this compound exhibited the highest inhibition of mushroom tyrosinase (Table 1).

To the best of our knowledge, our present study provides the first evidence that **2e** has a potent inhibitory effect on melanogenesis. First, we attempted to ascertain the potential cytotoxicity of **2e** on B16 cells. The cytotoxic effects of **2e** were estimated by measuring

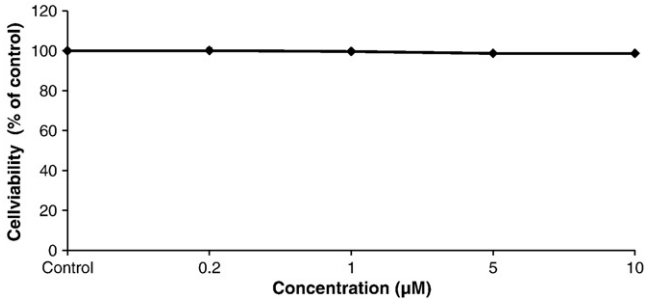

Fig. 3. Effect of **2e** on the cell viability of B16 cells. Cells were treated with various doses of **2e** (0–10 μM), and the effect of **2e** on the viability of B16 cells was examined by MTT assay. Data are expressed as percentage of control. $^{*}p<0.05$ compared to the untreated control.

Table 2
Effects on mushroom tyrosinase activity and kinetic analysis of compounds.

Compound	IC_{50}[a] (μM)	Kinetic analysis[b]						
		V_{max}	K_m (mM)			K_i (M)		
			1.25 μM	5.0 μM	20.0 μM	1.25 μM	5.0 μM	20.0 μM
2e	5.73 ± 1.40	1.75×10^{-2}	0.42	0.45	0.61	5.46×10^{-8}	1.95×10^{-7}	5.89×10^{-7}
Kojic acid	20.99 ± 1.80	–		–			–	

[a] 50% inhibitory concentration (IC_{50}).
[b] Lineweaver–Burk plot of mushroom tyrosinase: data are presented as mean values of 1/V, which is the inverse of the increase in absorbance at a wave-length 492 nm/min (ΔA_{492}/min), for three independent tests with different concentrations of L-tyrosine as the substrate.

cell viability, and no significant cytotoxic effect was found for any of the concentrations tested, as shown in Fig. 3. These results indicated that **2e** was relatively non-cytotoxic to cells under the experimental conditions used. As shown in Table 2, we examined the inhibitory action of **2e** on mushroom tyrosinase activity, and found that **2e** had a strong suppressive action on the enzyme, with an IC_{50} value of 5.73 ± 1.4 μM. Compared with kojic acid ($IC_{50} = 20.99 \pm 1.8$ μM), **2e** appeared to have a more powerful effect. The inhibitory efficacy of **2e** may be attributed to its hydroxyl and methoxy groups at R^2 and R^3 on the phenyl ring, respectively. The scaffold of **2e** was structurally similar to DOPA. To explore the inhibitory mechanism of **2e**, we conducted a study of the kinetic behavior of tyrosinase activity in the presence of **2e** (Table 2). As the concentration of **2e** increased, the K_m value of **2e** also increased gradually without changing V_{max}, thereby indicating that **2e** acts as a competitive inhibitor of mushroom tyrosinase. Tyrosinase is a copper-containing enzyme that is widely distributed in nature [46], and most tyrosinase inhibitors that chelate the copper in the active site of the enzyme show competitive inhibition; examples of such inhibitors are tropolone [47] and kojic acid [12]. Thus, the inhibition mechanism of **2e** might involve binding to the copper active site of mushroom tyrosinase. Therefore, we predicted the tertiary structure of mushroom tyrosinase and simulated its docking with **2e** using DOCK6. We searched for tyrosinase residues that might bind to compound **2e**, and found that the most important binding residues for interaction with **2e** are expected to be THR 195, ASP 262, HIS 265, VAL 266, SER 275, ASP 276, and PRO 277 (Fig. 4). These residues existed within 3 of the ligand. The docking simulation supported the slope-parabolic mixed-type inhibition observed, as this type of inhibition is generally encountered when there are multiple possible binding sites for an inhibitor. The docking simulation was successful, with significant scores using DOCK6 (binding energy: −26.79 kcal/mol), and suggested that it is mainly the PRO 96 residue that is responsible for the interaction with **2e**.

We also examined the inhibitory effect of **2e** on the tyrosinase activity of B16 cells treated with 100 nM α-MSH, and found that

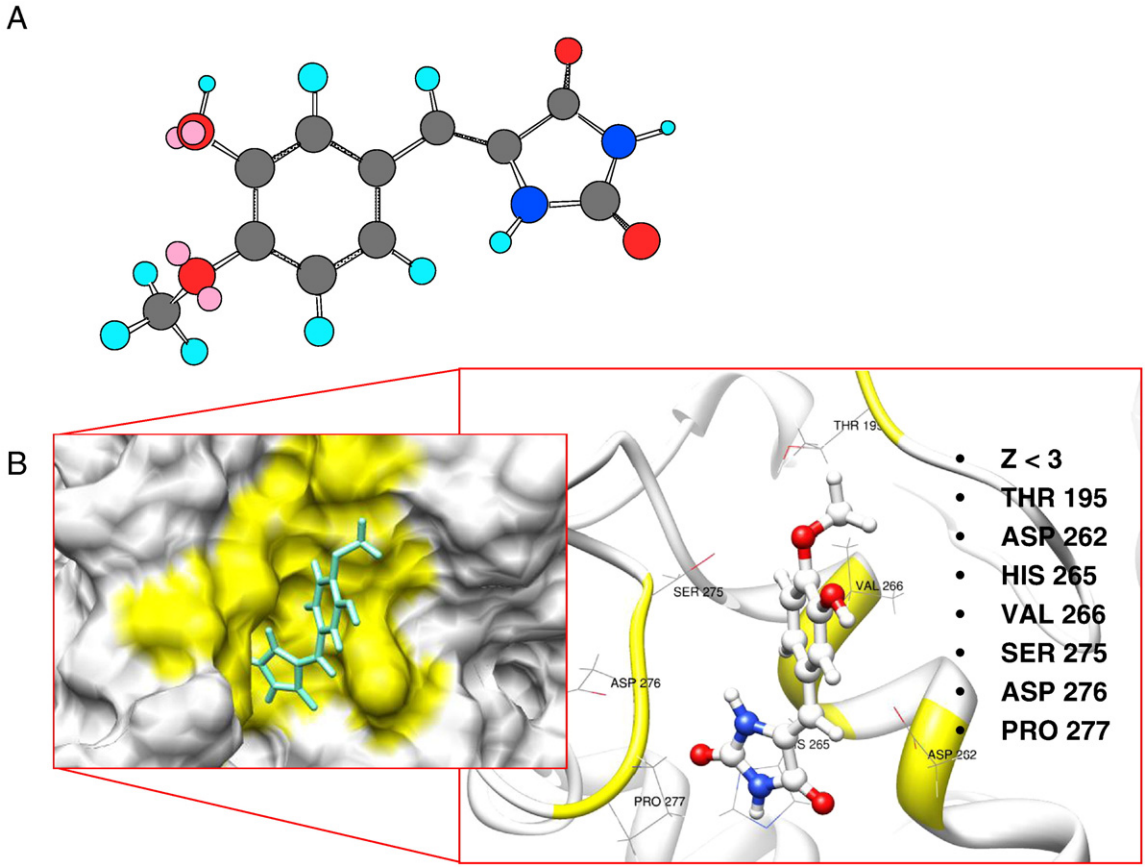

Fig. 4. Computational prediction of the structure for tyrosinase and docking simulation with **2e**. Predicted 3D structure of mushroom tyrosinase. A. Chemical structure of **2e**. B. The box indicates **2e** binding sites with tyrosinase residues THR 195, ASP 262, HIS 265, VAL 266, SER 275, ASP 276, and PRO 277. The yellow area interacts with the ligand ($Z < 3$).

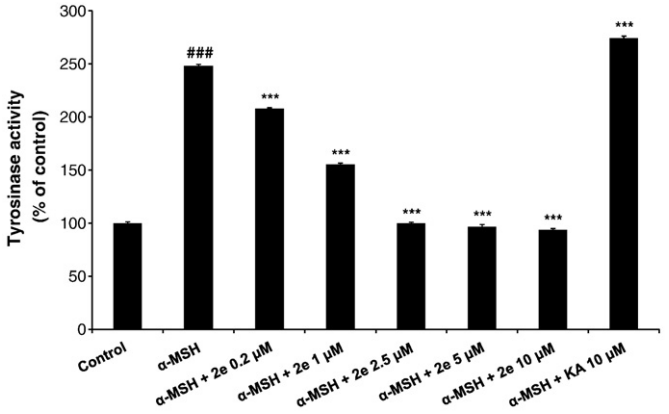

Fig. 5. Activity results of **2e** on B16 cell tyrosinase. In the presence of 100 nM MSH, B16 cells were treated with various doses of **2e** (0.2–0.0 μM) for 24 h. Results are expressed as percentage of control, and each column represents the mean ± S.E. of three determinations. $^{###}p<0.001$ compared to the untreated control, $^{***}p<0.001$ compared to the group treated with 100 nM α-MSH, KA (kojic acid).

2e inhibited the tyrosinase activity effectively compared to the α-MSH-treated group (Fig. 5). As the results show, the inhibitory effect of **2e** on tyrosinase activity was stronger than that of 10 μM kojic acid with 100 nM α-MSH-treated B16 cells. We also evaluated the melanin contents of cultured B16 cells in the presence of **2e** (ranging from 0.2 to 10 μM), and found that melanin synthesis was effectively inhibited in a dose-related manner, thereby supporting the mechanism by which **2e** inhibits the tyrosinase of B16 cells. The inhibitory effect of **2e** on melanin contents was stronger than that of 10 μM kojic acid with 100 nM α-MSH-treated B16 cells (Fig. 6). When the clog*P* values of hydantoin analog and the corresponding stilbene derivative are compared, hydantoin analog shows a little lower value. Therefore, hydantoin analogs may have better beneficial effect on manufacturing cosmetics with moisturizing ingredients.

4. Conclusion

The 5-(substituted benzylidene)hydantoin derivatives showed anti-tyrosinase inhibition effects. The best results were obtained for compound **2e**, which possessed a hydroxyl group at R^2 and a methoxy group at R^3 on the phenyl ring, respectively. This work will enhance understanding of the mechanism of tyrosinase inhibition and will contribute to the development of effective drugs against hyperpigmentation. Considering the tyrosinase inhibitory activities of the 5-(substituted benzylidene)hydantoin derivatives, the hydantoin template was thought to be a perfect surrogate for thiazolidine-carboxylic acid. This study indicates the possibility of the imide and amine groups acting as pharmacophores in tyrosinase inhibitors.

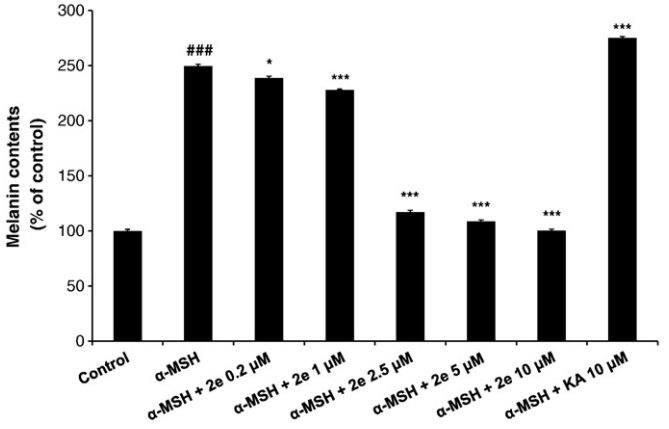

Fig. 6. The ability of **2e** to inhibit melanogenesis in the presence of 100 nM α-MSH in B16 cells. Melanin levels were measured at 405 nm. Values are the means ± S.E. of three experiments. Data are expressed as percentage of control. $^{###}p<0.001$ compared to the untreated control, $^{*}p<0.05$ and $^{***}p<0.001$ compared to the group treated with 100 nM α-MSH, KA, kojic acid.

Acknowledgments

This work was supported by a grant from the National Research Foundation of Korea (NRF) funded by the Korea government (MEST, No. 2009-0083538 and KRF-2008-314-E00292) and by the Basic Science Research Program through the National Research Foundation of Korea (NRF) funded by the Ministry of Education, Science and Technology (No. 2010-0012038). We also thank the Aging Tissue Bank for providing research materials for the study.

References

[1] C.J. Cooksey, P.J. Garratt, E.J. Land, S. Pavel, C.A. Ramsden, P.A. Riley, N.P. Smit, Evidence of the indirect formation of the catecholic intermediate substrate responsible for the autoactivation kinetics of tyrosinase, J. Biol. Chem. 272 (1997) 26226–26235.
[2] I. Kubo, I. Kinst-Hori, S.K. Chaudhuri, Y. Kubo, Y.T. Ogura, Flavonols from Heterotheca inuloides: tyrosinase inhibitory activity and structural criteria, Bioorg. Med. Chem. 8 (2000) 1749–1755.
[3] K. Urabe, J. Nakayama, Y. Hori, in: J.J. Norlund, R.E. Boissy, V.J. Hearing, R.A. King, J.P. Ortonne (Eds.), The Pigmentary System: Physiology and Pathophysiology, Oxford University Press, New York, 1998, pp. 909–911.
[4] M.K. Cullen, in: J.J. Norlund, R.E. Boissy, V.J. Hearing, R.A. King, J.P. Ortonne (Eds.), The Pigmentary System: Physiology and Pathophysiology, Oxford University Press, New York, 1998, pp. 760–766.
[5] S. Briganti, E. Camera, M. Picardo, Chemical and instrumental approaches to treat hyperpigmentation, Pigment Cell Res. 16 (2003) 101–110.
[6] D.S. Kim, S.Y. Kim, S.H. Park, Y.G. Choi, S.B. Kwon, M.K. Kim, J.I. Na, S.W. Youn, K.C. Park, Inhibitory effects of 4-n-butylresorcinol on tyrosinase activity and melanin synthesis, Biol. Pharm. Bull. 28 (2005) 2216–2219.
[7] S. Parvez, M. Kang, H.S. Chung, H. Bae, Naturally occurring tyrosinase inhibitors: mechanism and applications in skin health, cosmetics and agriculture industries, Phytother. Res. 21 (2007) 805–816.
[8] F. Solano, S. Briganti, M. Picardo, G. Ghanem, Hypopigmenting agents: an updated review on biological, chemical and clinical aspects, Pigment Cell Res. 19 (2006) 550–571.
[9] L. Lemic-Stoicevic, A.H. Nias, A.S. Breathnach, Effect of azelaic acid on melanoma cells in culture, Exp. Dermatol. 4 (1995) 79–81.
[10] J.R. Ros, J.N. Rodriguez-Lopes, F. Garcia-Canovas, Effect of L-ascorbic acid on the monophenolase activity of tyrosinase, Biochem. J. 295 (1993) 309–312.
[11] K. Maeda, M. Fukuda, Arbutin: mechanism of its depigmenting action in human melanocyte culture, J. Pharmacol. Exp. Ther. 276 (1996) 765–769.
[12] G. Battaini, E. Monzani, L. Casella, L. Santagostini, R. Pagliarin, Inhibition of the catecholase activity of biomimetic dinuclear copper complexes by kojic acid, J. Biol. Inorg. Chem. 5 (2000) 262–268.
[13] K. Ohguchi, T. Tanaka, T. Ito, M. Iinuma, K. Matsumoto, Y. Akao, Y. Nozawa, Inhibitory effects of resveratrol derivatives from dipterocarpaceae plants on tyrosinase activity, Biosci. Biotechnol. Biochem. 67 (2003) 1587–1589.
[14] N.H. Shin, S.Y. Ryu, E.J. Choi, S.H. Kang, I.M. Chang, K.R. Min, Y.S. Kin, Oxyresveratrol as the potent inhibitor on dopa oxidase activity of mushroom tyrosinase, Biochem. Biophys. Res. Commun. 243 (1998) 801–803.
[15] Y.M. Kim, J. Yun, C.K. Lee, H. Lee, K.R. Min, Y. Kim, Oxyresveratrol and hydroxystilbene compounds. Inhibitory effect on tyrosinase and mechanism of action, J. Biol. Chem. 277 (2002) 16340–16344.
[16] K. Ohguchi, T. Tanaka, I. Iliya, T. Ito, M. Iinuma, K. Matsumoto, Y. Akao, Y. Nozawa, Gnetol as a potent tyrosinase inhibitor from genus Gnetum, Biosci. Biotechnol. Biochem. 67 (2003) 663–665.
[17] J.S. Roh, J.Y. Han, J.H. Kim, J.K. Hwang, Inhibitory effects of active compounds isolated from safflower (*Carthamus tinctorius* L.) seeds for melanogenesis, Biol. Pharm. Bull. 27 (2004) 1976–1978.
[18] J.K. No, M.S. Kim, Y.J. Kim, S.J. Bae, J.S. Choi, H.Y. Chung, Inhibition of tyrosinase by protocatechuic aldehyde, Am. J. Chin. Med. 32 (2004) 97–103.
[19] Y. Kim, J. No, J. Lee, M. Kim, H. Chung, Antimelanogenic activity of 3,4-dihydroxyacetophenone: inhibition of tyrosinase and MITF, Biosci. Biotechnol. Biochem. 70 (2006) 532–534.
[20] Y.J. Kim, J.K. No, J.H. Lee, H.Y. Chung, 4,4'-Dihydroxybiphenyl as a new potent tyrosinase inhibitor, Biol. Pharm. Bull. 28 (2005) 323–327.
[21] Y.M. Ha, S.W. Chung, S.H. Song, H.S. Suh, H.Y. Chung, 4-(6-Hydroxy-2-naphthyl)-1,3-bezendiol: a potent, new tyrosinase inhibitor, Biol. Pharm. Bull. 30 (2007) 1711–1715.
[22] C. Carmi, A. Cavazzoni, V. Zuliani, A. Lodola, F. Bordi, P.V. Plazzi, 5-benzylidene-hydantoins as new EGFR inhibitors with antiproliferative activity, Bioorg. Med. Chem. Lett. 16 (2006) 4021–4025.

[23] S.S. Hah, H.M. Kim, R.A. Sumbad, P.T. Henderson, Hydantoin derivative formation from oxidation of 7,8-dihydro-8-oxo-2'-deoxyguanosine (8-oxodG) and incorporation of 14C-labeled 8-oxodG into the DNA of human breast cancer cells, Bioorg. Med. Chem. Lett. 15 (2005) 3627–3631.
[24] J. Chinnappa, P.T. Wong, W. Thenmozhiyal, K. Chui, Anticonvulsant activity of phenylmethylenehydantoins: a structure–activity relationship study, J. Med. Chem. 47 (2004) 1527–1535.
[25] K.I. Ahmed, Synthesis of arylidenehydrazono- and glycopyranosylhydrazinosulfonylbenzylidene-2,4-imidazolidinediones as potential antiviral and antitumoral agents, Carbohydr. Res. 306 (1998) 567–573.
[26] T.R. Rodgers, M.P. LaMontagne, A. Markovac, A.B. Ash, Hydantoins as antitumor agents, J. Med. Chem. 20 (1977) 591–594.
[27] R.N. Comber, R.C. Reynolds, J.D. Friedrich, R.A. Manguikian, R.W. Buckheit, J.J.W. Truss, 5,5-disubstituted hydantoins: syntheses and anti-HIV activity, J. Med. Chem. 35 (1992) 3567–3572.
[28] L. Somsak, L. Kovacs, M. Toth, E. Osz, L. Szilagyi, Z. Gyorgydeak, Synthesis of and a comparative study on the inhibition of muscle and liver glycogen phosphorylases by epimeric pairs of D-gluco- and D-xylopyranosylidene-spiro-(thio)hydantoins and N-(D-glucopyranosyl) amides, J. Med. Chem. 44 (2001) 2843–2848.
[29] C.W. Bazil, T.A. Pedley, Advances in the medical treatment of epilepsy, Annu. Rev. Med. 49 (1998) 135–162.
[30] M.S. Luer, Fosphenytoin, Neurol. Res. 20 (1998) 178–182.
[31] M. Matsukura, Y. Daiku, K. Ueda, S. Tanaka, T. Igarashi, N. Minami, Synthesis and antiarrhythmic activity of 2,2-dialkyl-1'-(N-substituted aminoalkyl)-spiro-(chroman-4,4'-imidazolidine)-2',5'-diones, Chem. Pharm. Bull. 40 (1992) 1823–1827.
[32] J. Knabe, J. Baldauf, A. Ahlhelm, Racemates and enantiomers of basic, substituted 5-phenylhydantoins, synthesis and anti-arrhythmic action, Pharmazie 52 (1997) 912–919.
[33] J.C. Menendez, M.P. Diaz, C. Bellver, M.M. Sollhuber, ChemInform abstract: synthesis, anticonvulsant and antihypertensive activity of diastereomeric 9,10-dimethoxy-1,3,4,6,7,11b-hexahydrospiro(benzo(a) quinolizin-2,4′-imidazolidine)-2′,5′-diones, Eur. J. Med. Chem. 27 (1992) 61–66.
[34] G.P. Moloney, A.D. Robertson, G.R. Martin, S. MacLennan, N. Mathews, S. Dosworth, A novel series of 2,5-substituted tryptamine derivatives as vascular 5HT1B/1D receptor antagonists, J. Med. Chem. 40 (1997) 2347–2362.
[35] G.P. Moloney, G.R. Martin, N. Mathews, A. Milne, H. Hobbs, S. Dosworth, Synthesis and serotonergic activity of substituted 2, N-benzylcarboxamido-5-(2-ethyl-1-dioxoimidazolidinyl)-N, N-dimethyltryptamine derivatives: novel antagonists for the vascular 5-HT(1B)-like receptor, J. Med. Chem. 42 (1999) 2504–2526.
[36] M. Jansen, H. Potschka, C. Brandt, W. Loscher, G. Dannhardt, Hydantoin-substituted 4,6-dichloroindole-2-carboxylic acids as ligands with high affinity for the glycine binding site of the NMDA receptor, J. Med. Chem. 46 (2003) 64–73.
[37] K. Last-Barney, W. Davidson, M. Cardozo, L.L. Frye, C.A. Grygon, J.L. Hopkins, Binding site elucidation of hydantoin-based antagonists of LFA-1 using multidisciplinary technologies: evidence for the allosteric inhibition of a protein–protein interaction, J. Am. Chem. Soc. 123 (2001) 5643–5650.
[38] C.S. Ananda Kumar, S.B. Benaka Prasad, K. Vinaya, S. Chandrappa, N.R. Thimmegowda, S.R. Ranganatha, S. Sanjay, K.S. Rangappa, Synthesis and antiproliferative activity of substituted diazaspiro hydantoins: a structure–activity relationship study, Invest. New Drugs 27 (2009) 131–139.
[39] H. Tada, O. Shiho, K. Kuroshima, M. Koyama, K. Tsukamoto, An improved colorimetric assay for interleukin 2, J. Immunol. Meth. 93 (1986) 157–165.
[40] J.K. No, D.Y. Soung, Y.J. Kim, K.H. Shim, Y.S. Jun, S.H. Rhee, T. Yokozawa, H.Y. Chung, Inhibition of tyrosinase by green tea components, Life Sci. 65 (1999) PL241–PL246.
[41] D.S. Kim, S.Y. Kim, J.H. Chung, K.H.H. Kim, C. Eun, K.C. Park, Delayed ERK activation by ceramide reduces melanin synthesis in human melanocytes, Cell. Signal. 14 (2002) 779–785.
[42] M.L. Bilodeau, J.D. Greulich, R.L. Hullinger, C. Bertolotto, R. Ballotti, O.M. Andrisani, BMP-2 stimulates tyrosinase gene expression and melanogenesis in differentiated melanocytes, Pigmen. Cell Res. 14 (2001) 328–336.
[43] K. Arnold, L. Bordoli, J. Kopp, T. Schwede, The SWISS-MODEL workspace: a web-based environment for protein structure homology modeling, Bioinformatics 22 (2006) 195–201.
[44] R. Rodriguez, G. Chinea, N. Lopez, T. Pons, G. Vriend, Homology modeling, model and software evaluation: three related resources, Bioinformatics 14 (1998) 523–528.
[45] D.T. Moustakas, P.T. Lang, S. Pegg, E. Pettersen, I.D. Kuntz, N. Brooijmans, R.C. Rizzo, Development and validation of a modular, extensible docking program: DOCK 5, J. Comput. Aided Mol. Des. 20 (2006) 601–619.
[46] V.J. Hearing, K. Tsukamoto, Enzymatic control of pigmentation in mammals, FASEB J. 5 (1991) 2902–2909.
[47] A. Andrawis, V. Kahn, Effect of methimazole on the activity of mushroom tyrosinase, Biochem. J. 235 (1986) 91–96.